AGU PUBLICATIONS

JGR

Journal of Geophysical Research: Space Physics

RESEARCH ARTICLE
10.1002/2015JA021370

Classifying onset durations of early VLF events: Scattered field analysis and new insights

D. A. Kotovsky[1] and R. C. Moore[1]

[1] Department of Electrical and Computer Engineering, University of Florida, Gainesville, Florida, USA

Key Points:
- VLF scattering
- Transient luminous events
- Ionospheric disturbances

Correspondence to:
D. A. Kotovsky,
dakotovsky@ufl.edu

Citation:
Kotovsky, D. A., and R. C. Moore (2015), Classifying onset durations of early VLF events: Scattered field analysis and new insights, *J. Geophys. Res. Space Physics*, *120*, 6661–6668, doi:10.1002/2015JA021370.

Received 30 APR 2015
Accepted 12 JUN 2015
Accepted article online 19 JUN 2015
Published online 4 AUG 2015

Abstract The physical processes responsible for a variety of early VLF scattering events have not yet been satisfactorily identified. Properly categorizing the early VLF event type is imperative to understand the causative physical processes involved. In this paper, the onset durations of 26 exceptionally high signal-to-noise ratio early VLF scattering events are analyzed, using scattered fields to classify events. New observations of events that exhibit "slow" amplitude changes, but "fast" scattered field changes are presented, which call into question previous analyses of early/slow events. We separately identify and analyze three early VLF events that definitively exhibit slow scattered field behavior. Additionally, we identify a significant number of events which have onset durations between the current definitions of fast and slow. Four events are observed which unambiguously exhibit a rapid initial rotation of the scattered field phasor during the first few seconds of the recovery stage. Possible physical mechanisms are discussed.

1. Introduction

Very low frequency (VLF, 3–30 kHz) radio waves are sensitive to changes in the electrical properties of the lower ionosphere, as they undergo reflection in the altitude range of 70 to 90 km. By means of this principle, man-made VLF transmissions have been utilized to remotely investigate a wide variety of cosmic, heliospheric, magnetospheric, and anthropogenic effects on the lower ionosphere, such as cosmic radiation [*Molder*, 1960], gamma radiation [*Inan et al.*, 1999], solar flares [*McRae and Thomson*, 2004], solar eclipses [*Clilverd et al.*, 2001], solar cycle variation [*Thomson and Clilverd*, 2000], diurnal variation [*McRae and Thomson*, 2000; *Thomson et al.*, 2007], VLF wave coupling to the magnetosphere [*Carpenter and Miller*, 1976], enhanced electron precipitation associated with magnetic substorms [*Potemra and Rosenberg*, 1973], high-altitude nuclear explosions [*Zmuda et al.*, 1963], and high-power, high-frequency radio wave heating [*Barr et al.*, 1985].

Only a few decades ago, *Armstrong* [1983] observed VLF amplitude perturbations within 100 ms of lightning discharges, implying a direct and immediate effect of the lightning discharge on the lower ionosphere (in contrast to the indirect and delayed effects of lightning-induced electron precipitation [*Helliwell et al.*, 1973]). Studies of these "early" VLF scattering events have since examined the relationship between lightning and the upper atmosphere by providing experimental observations in support of modeled conductivity changes associated with a variety of transient luminous events (TLEs) and by driving theoretical investigation of TLEs by demonstration of new and unexplained VLF event properties.

In this paper, we report that careful consideration must be taken for proper analysis of these lightning-induced VLF perturbations. We note that such considerations equally apply to the analysis of VLF perturbations associated with any transient ionospheric disturbance—such as those discussed above—common or uncommon to the dynamic Earth/space weather environment.

2. Background

Lightning discharges are capable of directly heating and ionizing the lower ionosphere via the produced quasi-electrostatic field changes and electromagnetic pulse radiation and have been associated with a variety of mesospheric TLEs including sprites [e.g., *Franz et al.*, 1990], elves [e.g., *Boeck et al.*, 1992], sprite halos [e.g., *Barrington-Leigh et al.*, 2001], and gigantic jets [e.g., *Pasko et al.*, 2002]. Under certain conditions, the ionospheric conductivity changes associated with TLEs can scatter subionospherically propagating VLF radio waves, resulting in early signal perturbations within ~20 ms of the causative lighting discharge [*Inan et al.*, 1993].

Preliminary observations of early VLF events exhibited high variability in onset duration [*Inan et al.*, 1988, 1995], defined as the time between the start of the event and the occurrence of the maximal amplitude/phase perturbation, ranging from ≤20 ms to ∼2 s. Since then, early event onset durations have been categorized as "fast" (onset duration ≤20 ms) [*Inan et al.*, 1996a] and "slow" (between ∼0.5 and ∼2.5 s) [*Haldoupis et al.*, 2004, 2006]. However, some studies after the work of *Inan et al.* [1996a] have utilized the term fast to describe events with slower onset durations of <50, <100, or 1000 ms [*Sampath et al.*, 2000; *Kumar et al.*, 2008; *Salut et al.*, 2013; *Marshall et al.*, 2014]. We note that elves, sprite halos, and sprites have been observed with optical durations less than 20 ms [e.g., *Stenbaek-Nielsen et al.*, 2000; *Stenbaek-Nielsen and McHarg*, 2008; *Newsome and Inan*, 2010]. Elves, specifically, are observed with optical durations on the order of tens of microseconds, and their modeled conductivity changes develop on that same time scale [*Taranenko et al.*, 1993]. While sprite halos have been observed to have optical durations on the order of milliseconds [*Stenbaek-Nielsen et al.*, 2000], their modeled conductivity changes may continue to develop up to and beyond 50 ms [*Liu*, 2012]. It is also accepted that the time scales of the lightning charge moment change affect the time dynamics of sprite halo development [e.g., *Li et al.*, 2012]. Additionally, sprite elements have been observed to exhibit optical durations up to 100 ms [*Stenbaek-Nielsen and McHarg*, 2008], implying conductivity changes developing on similar, if not longer, time scales. Even in the case of optically fast sprites, theoretical analysis suggests that prolonged conductivity development in sprite streamers could result in VLF onset durations of up to ∼100 ms [*Dowden et al.*, 2001a, 2001b]. In order to best relate observed VLF event properties to the time dynamics of conductivity changes associated with TLEs, it is imperative to perform VLF scattering observations with high time resolution. High signal-to-noise ratio (SNR) is also often required to properly quantify the onset duration (presenting a trade off between time resolution and SNR).

Additionally, we will demonstrate the necessity of scattered field analysis (i.e., simultaneous analysis of *both* amplitude *and* phase perturbations) for the proper characterization of VLF event onset durations. *Dowden et al.* [1997] and *Dowden and Rodger* [1997] demonstrated the necessity of scattered field analysis for proper characterization of VLF event recoveries by showing that the phasor addition of an ambient field and a logarithmically decaying scattered field can account for much of the complicated structure observed in the resulting amplitude and phase perturbations (e.g., events exhibiting a rapid initial amplitude recovery, a feature which has been otherwise attributed to a variety of speculated physical mechanisms [*Dowden et al.*, 1994; *Inan et al.*, 1996b; *Cotts and Inan*, 2007; *Haldoupis et al.*, 2013]). Scattered field analysis has also been applied to study both theoretical and experimental scattering patterns [*Johnson et al.*, 1999; *Moore et al.*, 2003].

Events which exhibit an amplitude-only or phase-only perturbation are not uncommonly observed and result from a normalized scattered field phase near 0/180° or 90/270°, respectively. Under these circumstances, the time dynamics of the normalized scattered field — and transitively, the ionospheric conductivity disturbance — are more readily understood from the time dynamics of the amplitude-only or phase-only perturbation. Since the modal content of the scattered field often differs appreciably from the modal content of the ambient field, the normalized scattered field angle varies spatially, such that a receiver in one location might observe an amplitude-only or phase-only perturbation, while a receiver in another location might observe simultaneous amplitude and phase perturbations.

Despite the clear strength of scattered field analysis, it has yet to be directly applied to rigorously interpret VLF event onset durations. In this context, it is worth noting that early/slow VLF events have been identified using only amplitude observations [*Haldoupis et al.*, 2006]. Of relevance, it has been suggested that cumulative ionization produced by multiple lightning strokes/discharges may have been responsible for observed slow onset durations [*Inan et al.*, 1995; *Haldoupis et al.*, 2006], supported by observations of multiple radio atmospherics (spherics) [*Inan et al.*, 1995] and spheric clusters occurring throughout the onset of early/slow amplitude perturbations [*Haldoupis et al.*, 2006]. The observations reported in this paper indicate that the occurrence of spherics needs to be associated with the temporal development of the scattered field magnitude, rather than with the temporal development of either the amplitude or the phase perturbations alone. Thus, the amplitude-only observations presented by *Inan et al.* [1995] and *Haldoupis et al.* [2006] need to reevaluated after considering scattered field analysis.

In this work, the scattered field analysis presented by *Dowden et al.* [1997] is extended and applied to high time resolution (20 ms) and high SNR data in order to rigorously characterize the onset durations of early

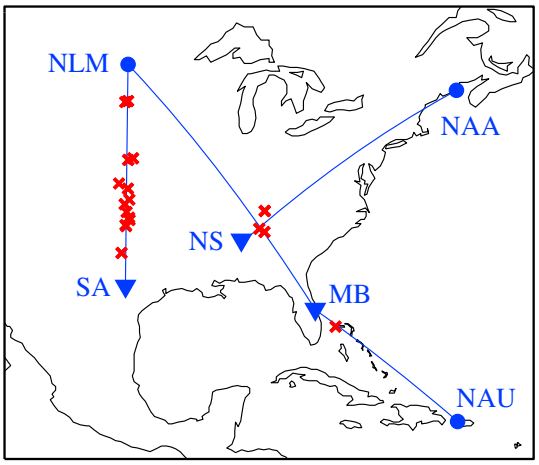

Figure 1. Map of transmitters NLM, NAA, and NAU (circles) and receivers MB, NS, and SA (triangles) with the 22 NLDN-recorded lightning return strokes.

VLF events. It is found that sole use of the observed amplitude or phase changes may lead to an incorrect or inconsistent characterization of the VLF event. By use of scattered field analysis, the existence of early/slow events is definitively confirmed. Furthermore, we identify a number of early events having onset durations between 20 and 100 ms, which may indicate that the current definition of fast is too restrictive or, alternatively, may point to distinct physical mechanisms. New observations of events exhibiting accelerated initial rotation of the scattered field phasor are presented, which to the authors knowledge have yet to be identified. In the final section, physical implications of our observations as they relate to known lightning-induced ionospheric disturbances are discussed.

3. Description of the Experiment

The signals broadcast by VLF transmitters NAA (24.0 kHz, Cutler, Maine), NLM (25.2 kHz, LaMoure, North Dakota), and NAU (40.75 kHz, Aguanda, Puerto Rico) are recorded at three receiver sites: Melbourne, Florida (MB, 28.06°N, 80.62°W); Tuscaloosa, Alabama (NS, 33.47°N, 87.63°W); and San Antonio, Texas (SA, 29.76°N, 98.57°W). Receiver systems consist of two orthogonal magnetic loop antennas, directed to geomagnetic north-south and east-west, a preamplifier, a line receiver, and a digitizing computer, with the exception of Melbourne, which contains only one loop antenna oriented to maximize the amplitude of the received NLM signal. Receivers are sensitive to magnetic fields in the frequency range of ~300 Hz to ~47 kHz. Signals are sampled at a rate of 100 kHz with 16-bit resolution, while accurate (100 ns absolute error) timing is provided by a GPS-trained oscillator with 10^{-12} frequency precision. The narrowband VLF transmitter signals are processed in real time and recorded separately with both 20 ms and 1 s resolution.

Observations of VLF amplitude and phase perturbations are identified as early events by association with radio atmospherics in broadband data. Twenty-six early events exhibiting both amplitude and phase perturbations with high "event SNR" (scattered field magnitude divided by root-mean-square noise) are analyzed. Data from the National Lightning Detection Network (NLDN) [*Orville*, 1991] is used to identify lightning flash location, polarity, and peak current, when possible. A map of the transmitter/receiver geometry, together with 22 NLDN-recorded lightning flashes (associated with 17 early VLF events), is shown in Figure 1. Of these causative discharges, all but four were positive polarity, and each resulted in a scattering angle of less than 11° to the receiver (assuming that the ionospheric disturbance is centered above the causative lightning discharge).

The total field arriving at the receiver during a VLF event is considered to be a superposition of the ambient field and the net field scattered by the ionospheric disturbance. After estimating the ambient field via linear interpolation between the preonset and postrecovery ambient fields, the normalized scattered field is calculated using the phasor geometry shown in Figure 2. Note that this method requires no knowledge of involved scattering parameters (e.g., ionospheric disturbance geometry, path geometries, and Earth-ionosphere waveguide properties). Uncertainty in the ambient field estimation during the event has minimal impact on the evaluation of onset durations, as the preevent ambient fields are known precisely, and ambient fields change minimally on the time scales of the onset durations considered here (tens of milliseconds to a few seconds). During the perturbation recovery (order of minutes or greater), the ambient field can alter appreciably, meaning that the choice of recovery estimation technique can greatly affect the calculated recovery time (see discussion in *Dowden et al.* [2001a]). This study is concerned only with the first few seconds of recovery, smaller than the typical time scales of natural ionospheric variation. In order to analyze

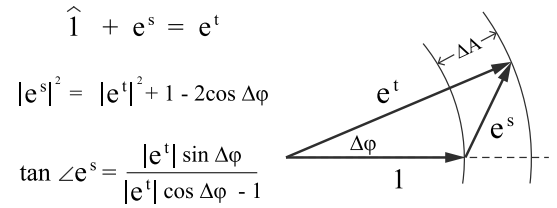

Figure 2. Phasor diagram showing how the normalized total field phasor (e^t) and normalized scattered field phasor (e^s) are calculated given the measured amplitude and phase perturbations (ΔA and $\Delta\phi$, respectively). All field values are normalized by the estimated ambient field (i.e., the normalized ambient field is unity).

scattered field dynamics in particular, we restrict our data set to large events that exhibit both amplitude and phase perturbations.

For clarity, throughout this paper we will use the terminology of event amplitude and phase perturbations, and scattered field magnitude and angle.

4. Experimental Observations

Four exemplary events (at 20 ms resolution) are shown in Figure 3. Narrowband amplitude and phase data are shown in Figure 3 (top row), normalized scattered field magnitude and angle data are shown in Figure 3 (middle row), and uncalibrated broadband data (10 μs resolution) are shown in Figure 3 (bottom row). Event types are here characterized by the onset durations of the scattered field magnitudes.

Figure 3a (with a scattered field magnitude, $|e^s|$, uncertainty of ± 0.035; a scattered field angle, $\angle e^s$, uncertainty of ± 5.3°; and 21 dB event SNR) demonstrates a traditional early/fast perturbation, with a fast (<20 ms) rise time for the scattered field magnitude as well as for the amplitude and phase perturbations (for clarity, dots are placed on data points near to and including the onset duration). In most cases, the scattered field magnitude and angle exhibit continuous and approximately logarithmic recoveries (true for Figures 3a–3d). The majority of analyzed events (15 out of 26) exhibit fast scattered field onset durations coincident with a single spheric, although in 9 of these 15 cases, the resulting amplitude and phase perturbations are not *simultaneously* fast. For two events exhibiting a <60 ms onset duration (see Figure 3c below), either the amplitude or phase perturbation exhibits an exceptionally slow (> 500 ms) onset duration, due to the nuances of phasor addition.

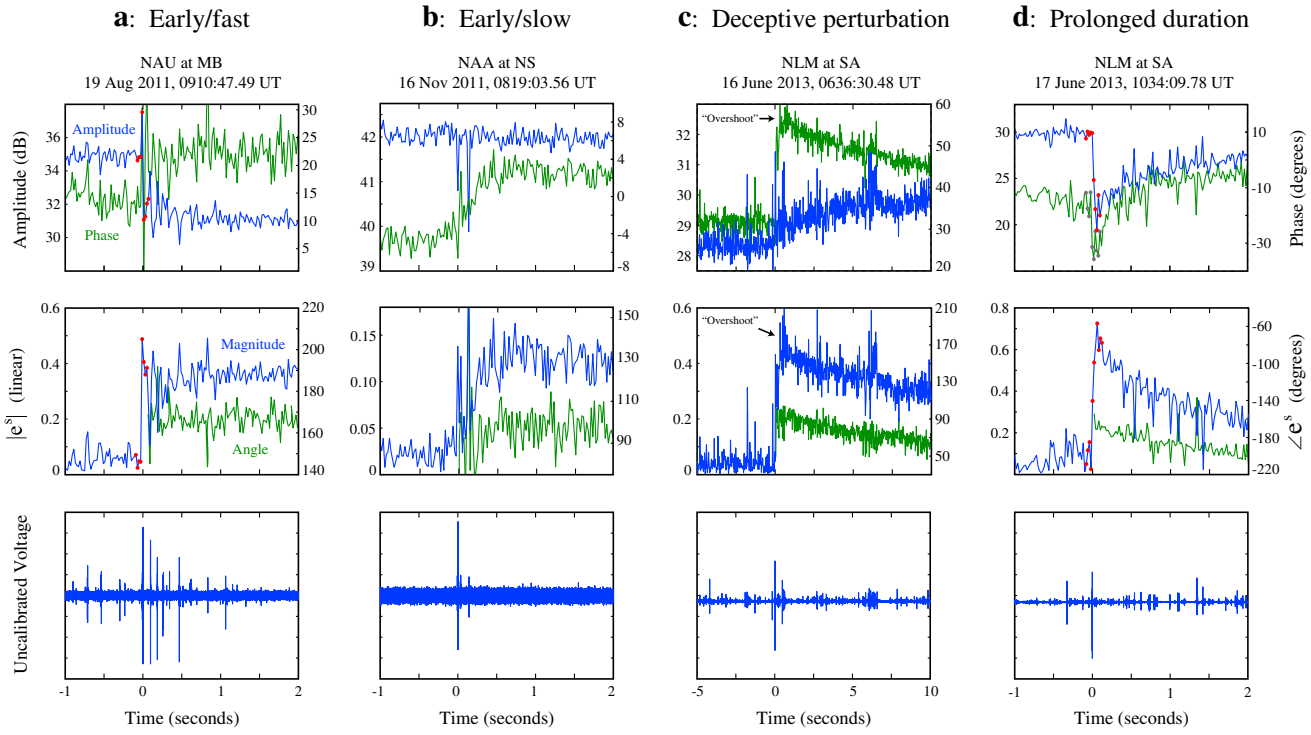

Figure 3. Early VLF events: (a) traditional early/fast, (b) traditional early/slow, (c) fast scattered field with slow amplitude changes, and (d) prolonged onset duration. (top row) 20 ms resolution amplitude (blue trace) and phase (green trace), (middle row) normalized scattered field magnitude (blue) and angle (green), and (bottom row) uncalibrated broadband data (10 μs resolution) for spheric detection. See text for estimated error.

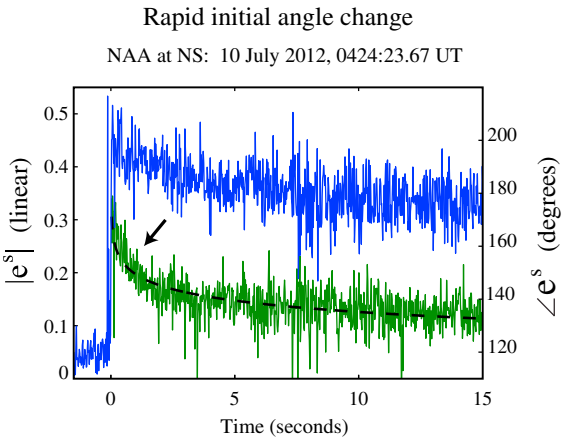

Figure 4. Normalized scattered field magnitude (blue trace) and angle (green) for an accelerated initial rotation early VLF event, with the angle exhibiting an exceptionally sharp logarithmic dependence (fit shown by dashed line). Estimated error: scattered field magnitude, ± 0.057; scattered field angle, ± 7.8°; 17 dB event SNR.

A typical early/slow event is demonstrated by Figure 3b ($|e^s|$ ± 0.032; $\angle e^s$ ± 15.7°; 11 dB SNR), for which the scattered field and the resulting amplitude/phase perturbations exhibit rise times of ~0.5 s. For the three early/slow events observed, multiple spherics occurred during the event onset duration (as shown in Figure 3 (bottom row)). Two of these three events (not shown) have associated NLDN data, showing multiple, distinct lightning flashes grouped within 1.4 km of each other in one case, and within 53 km in the other case. In the former case, the scattered field continues to increase in magnitude for over a second after the last detected spheric or NLDN flash, implying the event results from a slowly developing causative physical mechanism, rather than from the cumulative effects of multiple fast processes.

Figure 3c ($|e^s|$ ± 0.039; $\angle e^s$ ± 5.2°; 21 dB SNR) resulted in an amplitude perturbation that takes ~7.5 s to reach its maximal change (note the 10 s time scale used in the figure). The temporal characteristics of the normalized scattered field follow that of the phase perturbation: a sharp <60 ms rise, followed by an ~0.5 s slow growth "overshoot." The apparent discrepancy between the rise times of the resulting amplitude and phase perturbations can be understood via the phasor addition of the ambient and scattered fields: at the onset, the normalized scattered field angle is ~90°, resulting in a large phase perturbation only. As the scattered field decays, the normalized angle reduces (to ~70° after 7.5 s), leading to a slowly developing amplitude perturbation. We note that for the two events of this kind, only one spheric was detected during the scattered field onset durations. However, additional spherics were observed throughout the slower of the amplitude or phase perturbations that resulted. If these events had been incorrectly categorized as slow, one might have concluded that multiple spherics were involved in producing the events.

Figure 3d ($|e^s|$ ± 0.039; $\angle e^s$ ± 9.7°; 15 dB SNR) consists of scattered field and amplitude/phase changes with rise times between 20 and 60 ms. Although outside of the current technical definition of fast (≤20 ms), the rapid onset duration is distinct from those of slow events (~0.5 to 2.5 s). Eight events of this kind were observed; three with onset durations between 20 and 40 ms, four between 40 and 60 ms, and one between 80 and 100 ms. For each event, the prolonged scattered field onset duration also manifested in the resulting amplitude and phase perturbations. Additionally, for all but two of these events, only one spheric was detected during the scattered field onset duration.

Most events exhibit scattered field magnitudes and angles that recover continuously and approximately logarithmically with time, in agreement with past observation [*Dowden et al.*, 2001a]. In general, the scattered field angle decreases during the recovery (clockwise phasor rotation); however, two events exhibited an increasing angle (counterclockwise phasor rotation). Additionally, some events exhibit an angle with an exceptionally sharp logarithmic dependence relative to their slower and more gradual magnitude decay (i.e., a rapid initial rotation of the scattered field phasor). Our best example ($|e^s|$ ± 0.057; $\angle e^s$ ± 7.8°; 17 dB SNR) is shown in Figure 4 (with a logarithmic fit shown by a dashed line), to be compared with the events in Figure 3. Four events of this kind are unambiguously identified, exhibiting scattered field angle changes of +15, −24, −24, and −34°within the first three seconds of recovery, during which the magnitude remains above 80% of its peak value.

5. Discussion

In this work, we analyzed 26 early VLF events: 15 early/fast events, 9 of which do not have simultaneously fast amplitude and phase perturbations; 3 early/slow events; and 8 early events with onset durations in the range of 20 ms to 100 ms. Based on the observations of "deceptive" events (for which the amplitude and phase perturbations develop on distinctly different time scales) presented in Figure 3c, we conclude that the sole

use of amplitude or phase perturbations may lead to inconsistent and misleading characterizations of early VLF events and that scattered field analysis is essential to relate the characteristics of early VLF perturbations to underlying physical mechanisms.

We note that all observations of early/slow perturbations to date [*Inan et al.*, 1988, 1995; *Haldoupis et al.*, 2004, 2006] have employed solely amplitude observations; as such, the analysis performed here provides definitive evidence that early/slow VLF events exist. It may be the case that for some early/slow events, subsequent ionization from multiple lightning strokes/discharges builds up over the course of the onset duration, as proposed by *Inan et al.* [1995] and *Haldoupis et al.* [2006]. However, the observation of a slow onset duration continuing for over one second after the last detected spheric or NLDN flash indicates the occurrence of a physical process which develops over long time scales greater than hundreds of milliseconds, which may or may not be occurring for all early/slow events. Such event dynamics might be the experimental observation of the conductivity changes produced by persistent quasi-electrostatic fields at ionospheric altitudes due to continuing currents and/or *M* components, thereby relating to the development of sprites and/or sprite halos (but not elves).

Eight early VLF events were observed that have scattered field onset durations in the range of 20 ms to 100 ms. These might be explainable by a similar, physically slow mechanism as discussed for early/slow events, which suggests that there may be a continuum of onset durations between the current definitions of fast and slow. Such a continuum may be produced by prolonged conductivity development in sprite halos [*Liu*, 2012] or sprites [*Stenbaek-Nielsen et al.*, 2000; *Dowden et al.*, 2001a, 2001b]. Alternatively, there may be distinct physical processes leading to separate domains of onset durations (e.g., "<100 ms fast" and slow). Regardless, the existence of events with "prolonged" onset durations demonstrates the necessity of high time resolution (<20 ms) VLF observations in order to delineate among events with potentially distinct physical causative mechanisms.

Lastly, four events are observed which exhibit a scattered field angle with an exceptionally sharp logarithmic time dependence relative to their magnitude decay (see Figure 4). Such events may be due to an ionospheric disturbance whose geometry is changing significantly within the first seconds of recovery, altering the excitation of scattered field modes within the Earth-ionosphere waveguide. For example, in possible cases of VLF sprite scattering the shrinking columns of ionization have been modeled to produce a similar change in scattered field phase on the observed time scales [*Nunn and Rodger*, 1999].

Definitive observations of VLF scattering from gigantic jets (GJs) have been presented by *Marshall et al.* [2014]. However, the 1 s time resolution presented therein does not allow for classification of either the onset delay (i.e., early) or the onset duration (i.e., fast/slow). Until further quantification is available regarding the conductivity changes associated with GJs and the time scales on which they develop, the VLF onset delays and onset durations associated with gigantic jets are highly uncertain. Optical studies have shown that leading jets, reaching up to 90 km, develop on time scales ranging from <34 ms to ≥230 ms [*Pasko et al.*, 2002; *Su et al.*, 2003], implying that GJ VLF scattering might not necessarily be fast relative to the leading jet spheric. Additionally, fully developed leading jets have been observed to persist anywhere from <17 ms up to 167 ms, and durations of the total GJ (including trailing jets) can persist for many hundreds of milliseconds [*Pasko et al.*, 2002; *Su et al.*, 2003]. Given this wide range of optical durations, potential GJ VLF event onset durations could range anywhere from fast to slow (hundreds of milliseconds). Additionally, onset delay and onset duration will be affected by which portions of the GJ that contribute to VLF scattering. We note that the recent modeling efforts of *Lehtinen and Inan* [2007] demonstrated the production of long-lasting negative ion enhancements by GJs; however, the total conductivity changes were too small to efficiently scatter VLF radio waves.

The total scattered field observed may be a summation of fields scattered from numerous, co-occurring ionospheric disturbances (e.g., sprite with halo/elve), such that the effects from the mechanisms proposed above may compete or cooperate. Additionally, in the case of lower SNR VLF events, the onset time dynamics which relate directly to the development of the ionospheric disturbance may be too weak relative to the noise to be apparent. Of the few hundred distinct early VLF events cleanly observed at the three receivers over the course of about 2.5 years, we note that the majority are early/fast. The variety of possible and potentially competing mechanisms for events with onsets >20 ms calls for a large statistical survey of onset duration variability, which may help to clarify the important physical processes at play.

Acknowledgments
This work is supported by DARPA grant HR0011-10-1-0061 and by NSF grant PLR-1246275 to the University of Florida. The data used in this paper may be obtained by contacting Robert Moore (moore@ece.ufl.edu).

M. Balikhin thanks two anonymous reviewers for their assistance in evaluating this paper.

References

Armstrong, W. C. (1983), Recent advances from studies of the Trimpi effect, *Antarct. J. U. S.*, *18*, 281–283.
Barr, R., M. T. Rietveld, P. Stubbe, and H. Kopka (1985), The diffraction of VLF radio waves by a patch of ionosphere illuminated by a powerful HF transmitter, *J. Geophys. Res.*, *90*(A3), 2861–2875.
Barrington-Leigh, C. P., U. S. Inan, and M. Stanley (2001), Identification of sprites and elves with intensified video and broadband array photometry, *J. Geophys. Res.*, *106*(A2), 1741–1750, doi:10.1029/2000JA000073.
Boeck, W. L., O. H. Vaughan Jr., R. Blakeslee, B. Vonnegut, and M. Brook (1992), Lightning-induced brightening in the airglow layer, *Geophys. Res. Lett.*, *19*(2), 99–102.
Carpenter, D. L., and T. R. Miller (1976), Ducted magnetospheric propagation of signals from the Siple, Antarctica, VLF transmitter, *J. Geophys. Res.*, *81*(16), 2692–2700.
Clilverd, M. A., C. J. Rodger, N. R. Thomson, J. Lichtenberger, P. Steinbach, P. Cannon, and M. J. Angling (2001), Total solar eclipse effects on VLF signals: Observations and modeling, *Radio Sci.*, *36*(4), 773–788.
Cotts, B. R. T., and U. S. Inan (2007), VLF observation of long ionospheric recovery events, *Geophys. Res. Lett.*, *34*, L14809, doi:10.1029/2007GL030094.
Dowden, R. L., and C. J. Rodger (1997), Decay of a vertical plasma column: A model to explain VLF sprites, *Geophys. Res. Lett.*, *24*(22), 2765–2768, doi:10.1029/97GL02822.
Dowden, R. L., C. D. D. Adams, J. B. Brundell, and P. E. Dowden (1994), Rapid onset, rapid decay (RORD), phase and amplitude perturbations of VLF subionospheric transmissions, *J. Atmos. Terr. Phys.*, *56*(11), 1513–1527, doi:10.1016/0021-9169(94)90118-X.
Dowden, R. L., J. B. Brundell, and C. J. Rodger (1997), Temporal evolution of very strong Trimpis observed at Darwin, Australia, *Geophys. Res. Lett.*, *24*(19), 2419–2422.
Dowden, R., C. Rodger, J. Brundell, and M. Clilverd (2001a), Decay of whistler-induced electron precipitation and cloud-ionosphere electrical discharge Trimpis: Observations and analysis, *Radio Sci.*, *36*(1), 151–169, doi:10.1029/1999RS002297.
Dowden, R., C. Rodger, and D. Nunn (2001b), Minimum sprite plasma density as determined by VLF scattering, *IEEE Antennas Propag. Mag.*, *43*(2), 12–24, doi:10.1109/74.924600.
Franz, R. C., R. J. Nemzek, and J. R. Winckler (1990), Television image of a large upward electrical discharge above a thunderstorm system, *Science*, *249*(4964), 48–51.
Haldoupis, C., T. Neubert, U. S. Inan, A. Mika, T. H. Allin, and R. A. Marshall (2004), Subionospheric early VLF signal perturbations observed in one-to-one association with sprites, *J. Geophys. Res.*, *109*, A10303, doi:10.1029/2004JA010651.
Haldoupis, C., R. J. Steiner, A. Mika, S. Shalimov, R. A. Marshall, U. S. Inan, T. Bosinger, and T. Neubert (2006), "Early/slow" events: A new category of VLF perturbations observed in relation with sprites, *J. Geophys. Res.*, *111*, A11321, doi:10.1029/2006JA011960.
Haldoupis, C., M. Cohen, E. Arnone, B. Cotts, and S. Dietrich (2013), The VLF fingerprint of elves: Step-like and long-recovery early VLF perturbations caused by powerful ±CG lightning EM pulses, *J. Geophys. Res. Space Physics*, *118*, 5392–5402, doi:10.1002/jgra.50489.
Helliwell, R. A., J. P. Katsufrakis, and M. L. Trimpi (1973), Whistler-induced amplitude perturbation in VLF propagation, *J. Geophys. Res.*, *78*(22), 4679–4688.
Inan, U. S., D. C. Shafer, W. Y. Yip, and R. E. Orville (1988), Subionospheric VLF signatures of nighttime D region perturbations in the vicinity of lightning discharges, *J. Geophys. Res.*, *93*(A10), 11,455–11,472, doi:10.1029/JA093iA10p11455.
Inan, U. S., J. V. Rodriguez, and V. P. Idone (1993), VLF signatures of lightning-induced heating and ionization of the nighttime D-region, *Geophys. Res. Lett.*, *20*(21), 2355–2358, doi:10.1029/93GL02620.
Inan, U. S., T. F. Bell, V. P. Pasko, D. D. Sentment, E. M. Wescott, and W. A. Lyons (1995), VLF signatures of ionospheric disturbances associated with sprites, *Geophys. Res. Lett.*, *22*(24), 3461–3464, doi:10.1029/95GL03507.
Inan, U. S., V. P. Pasko, and T. F. Bell (1996a), Sustained heating of the ionosphere above thunderstorms as evidenced in "early/fast" VLF events, *Geophys. Res. Lett.*, *23*(10), 1067–1070, doi:10.1029/96GL01360.
Inan, U. S., A. Slingeland, V. P. Pasko, and J. V. Rodriguez (1996b), VLF and LF signatures of mesospheric/lower ionospheric response to lightning discharges, *J. Geophys. Res.*, *101*(A3), 5219–5238, doi:10.1029/95JA03514.
Inan, U. S., N. G. Lehtinen, S. J. Lev-Tov, M. P. Johnson, T. F. Bell, and K. Hurley (1999), Ionization of the lower ionosphere by γ-rays from a Magnetar: Detection of low energy (3–10 keV) component, *Geophys. Res. Lett.*, *26*(22), 3357–3360.
Johnson, M. P., U. S. Inan, S. J. Lev-Tov, and T. F. Bell (1999), Scattering pattern of lightning-induced ionospheric disturbances associated with early/fast VLF events, *Geophys. Res. Lett.*, *26*(15), 2363–2366, doi:10.1029/1999GL900521.
Kumar, S, A. Kumar, and C. J. Rodger (2008), Subionospheric early VLF perturbations observed at Suva: VLF detection of red sprites in the day?, *J. of Geophys. Res.*, *113*, A03311, doi:10.1029/2007JA012734.
Lehtinen, N. G., and U. S. Inan (2007), Possible persistent ionization caused by giant blue jets, *Geophys. Res. Lett.*, *34*, L08804, doi:10.1029/2006GL029051.
Li, J., S. Cummer, G. Lu, and L. Zigoneanu (2012), Charge moment change and lightning-driven electric fields associated with negative sprites and halos, *J. Geophys. Res.*, *117*, A09310, doi:10.1029/2012JA017731.
Liu, N. (2012), Multiple ion species fluid modeling of sprite halos and the role of electron detachment of O^- in their dynamics, *J. Geophys. Res.*, *117*, A03308, doi:10.1029/2011JA017062.
Marshall, R. A., T. Adachi, R.-R. Hsu, and A. B. Chen (2014), Rare examples of early VLF events observed in association with ISUAL-detected gigantic jets, *Radio Sci.*, *49*, 36–43, doi:10.1002/2013RS005288.
McRae, W. M., and N. R. Thomson (2000), VLF phase and amplitude: Daytime ionospheric parameters, *J. Atmos. Sol. Terr. Phys.*, *62*, 609–618.
McRae, W. M., and N. R. Thomson (2004), Solar flare induced ionospheric D-region enhancements from VLF phase and amplitude observations, *J. Atmos. Sol. Terr. Phys.*, *66*, 77–87.
Molder, W. F. (1960), VLF propagation effects of a D-region layer produced by cosmic rays, *J. Geophys. Res.*, *65*(5), 1459–1468.
Moore, R. C., C. P. Barrington-Leigh, U. S. Inan, and T. F. Bell (2003), Early/fast VLF events produced by electron density changes associated with sprite halos, *J. Geophys. Res.*, *108*(A10), 1363, doi:10.1029/2002JA009816.
Newsome, R. T., and U. S. Inan (2010), Free-running ground-based photometric array imaging of transient luminous events, *J. Geophys Res.*, *115*, A00E41, doi:10.1029/2009JA014834.
Nunn, D., and C. J. Rodger (1999), Modeling the relaxation of red sprite plasma, *Geophys. Res. Lett.*, *26*(21), 3293–3296.
Orville, R. E. (1991), Calibration of a magnetic direction finding network using measured triggered lightning return stroke peak currents, *J. Geophys. Res.*, *96*(D9), 17,135–17,142.
Pasko, V. P., M. A. Stanley, J. D. Mathews, U. S. Inan, and T. G. Woods (2002), Electrical discharge from a thundercloud top to the lower ionosphere, *Nature*, *416*, 152–154, doi:10.1038/416152a.
Potemra, T. A., and T. J. Rosenberg (1973), VLF propagation disturbances and electron precipitation at mid-latitudes, *J. Geophys. Res.*, *78*(10), 1572–1580.

Salut, M. M., M. B. Cohen, M. A. M. Ali, K. L. Graf, B. R. T. Cotts, and S. Kumar (2013), On the relationship between lightning peak current and Early VLF perturbations, *J. Geophys. Res. Space Physics*, *118*, 7272–7282, doi:10.1002/2013JA019087.

Sampath, H. T., U. S. Inan, and M. P. Johnson (2000), Recovery signatures and occurrence properties of lightning-associated subionospheric VLF perturbations, *J. Geophys. Res.*, *105*(A1), 183–191.

Stenbaek-Nielsen, H. C., D. R. Moudry, E. M. Wescott, D. D. Sentman, and F. T. Sao Sabbas (2000), Sprites and possible mesospheric effects, *Geophys. Res. Lett.*, *27*(23), 2829–3932, doi:10.1029/2000GL003827.

Stenbaek-Nielsen, H. C., and M. G. McHarg (2008), High time-resolution sprite imaging: Observations and implications, *J. Phys. D Appl. Phys.*, *41*, 234009, doi:10.1088/0022-3727/41/23/234009.

Su, H. T., R. R. Hsu, A. B. Chen, Y. C. Wang, W. S. Hsiao, W. C. Lai, L. C. Lee, M. Sato, and H. Fukunishi (2003), Gigantic jets between a thundercloud and the ionosphere, *Nature*, *423*, 974–976.

Taranenko, Y. N., U. S. Inan, and T. F. Bell (1993), Interaction with the lower ionosphere of electromagnetic pulses from lightning: Heating, attachment, and ionization, *Geophys. Res. Lett.*, *20*(15), 1539–1542.

Thomson, N. R., and M. A. Clilverd (2000), Solar cycle changes in daytime VLF subionospheric attenuation, *J. Atmos. Sol. Terr. Phys.*, *62*, 601–608.

Thomson, N. R., M. A. Clilverd, and W. M. McRae (2007), Nighttime ionospheric D region parameters from VLF phase and amplitude, *J. Geophys. Res.*, *112*, A07304, doi:10.1029/2007JA012271.

Zmuda, A. J., B. W. Shaw, and C. R. Haave (1963), Very low frequency disturbances and the high-altitude nuclear explosion of July 9, 1962, *J. Geophys. Res.*, *68*(3), 745–758.